Doping PbSe nanocrystals: Predictions based on a trapped-dopant model

Steven C. Erwin
Center for Computational Materials Science, Naval Research Laboratory, Washington, DC 20375, USA
(Received 25 January 2010; revised manuscript received 24 May 2010; published 25 June 2010)

We recently proposed that impurity doping in colloidally grown semiconductor nanocrystals is often controlled primarily by kinetics rather than by thermodynamics. In this "trapped-dopant" model the diffusion of an impurity through a nanocrystal is negligible at colloidal growth temperatures. Consequently, an impurity can only be incorporated as a dopant into a growing nanocrystal if it first adsorbs on the surface and is then overgrown. This surface adsorption can be complicated by a competing process: the binding of the impurity by surfactant molecules and other agents added to the growth solution to passivate the nanocrystal and control its growth. Here we use density-functional theory to study the interplay and outcome of these processes for the doping of PbSe nanocrystals by a number of candidate dopants (Mn, Co, Cl, In, Cd, Tl, etc.) in the presence of two widely used growth additives (oleic acid and hexadecylamine). The results suggest that successful doping requires making a trade-off between surface adsorption (which favors small dopants) and interior trapping (which favors large dopants). Moreover, the widely used growth agent oleic acid binds strongly to almost all dopants, suggesting that the standard growth procedure may require modification for successful doping to be realized.

DOI: 10.1103/PhysRevB.81.235433 PACS number(s): 61.72.S−, 61.46.Df, 81.07.Bc, 66.30.Pa

I. INTRODUCTION

The ability to add intentional impurities to a material at a specified concentration is so important, and for this reason so commonplace, that it is often taken for granted. Doping of semiconductor materials in bulk form is routinely performed during the growth, by adding impurities to the melt, or afterward, using diffusion or ion implantation. Successful dopant-host systems are well known for the technologically important semiconductors: phosphorous and boron dopants for doping silicon; silicon for doping gallium arsenide and gallium nitride; and so forth.

The doping of semiconductors in nanocrystalline form, however, is at a much earlier stage of development. Many early efforts to dope colloidally grown nanocrystals during their synthesis failed for reasons that were not clear. More recent efforts have been successful but these same successes have revealed new puzzles. Most striking is the very weak, or even absent, correspondence between the solubility of dopants in bulk crystals versus nanocrystals. For example, Mn dopant concentrations attained in ZnSe nanocrystals are one to two orders of magnitude lower than in bulk ZnSe.[1] On the other hand, Mn concentrations in InAs and InP nanocrystals are three to four orders of magnitude *higher* than in bulk.[2,3] Finally, Mn concentrations in ZnO nanocrystals are close to the solubility limit in bulk ZnO.[4]

The early failures to incorporate dopants into nanocrystals gave rise to the idea of a general "self-purification" mechanism that expels dopants from nanocrystals. But subsequent experiments,[2,3] which show dopant concentrations in nanocrystals much higher than in bulk, suggest a more complicated situation. The origin of these complications is the subject of an ongoing discussion[5–10] whose eventual resolution is essential for making doped nanoscale semiconductors viable as technological materials.

In this paper a recently developed "trapped-dopant" model of doping in nanocrystals[6,11,12] is used to explore, with first-principles total-energy calculations, the implications for doping nanocrystals of a specific semiconductor material, lead selenide. This exploration consists of a search for promising candidate dopants, in the limited sense of identifying dopants that are likely to be easily incorporated and physically stable in PbSe nanocrystals. The question of which dopants are predicted to behave as donors or acceptors is deferred to a later work.

This paper is organized as follows. The justification and main ideas of the trapped-dopant model are summarized in Sec. II. A short discussion is given in Sec. III of why PbSe nanocrystals are of interest and of which candidate dopants will be considered here. Three aspects of the model—trapping of dopants, adsorption of dopants, and competition for dopants—are explored computationally in Secs. IV–VI. Section VII addresses the "bottom line" by identifying which candidates are most promising as dopants for PbSe nanocrystals.

II. TRAPPED DOPANT MODEL

A. Thermodynamics vs kinetics

To formulate a realistic theory describing the incorporation of dopants in semiconductor nanocrystals it is useful to consider two very different starting points: thermodynamics and kinetics. By thermodynamics is meant here a description appropriate to a system in thermodynamic equilibrium. In this scenario a system remains at, or close to, its energetic ground state. This has long been a very illuminating starting point for both understanding and predicting theoretically the solubility of dopants in bulk semiconductors. It is simple to show that the host+dopant system minimizes its free energy when the relative concentration of dopants x_{imp} is equal to the Boltzmann factor, $\exp(-E_{\mathrm{form}}/kT)$. The impurity formation energy E_{form} is the difference between the internal energy of two systems: one in which the impurity is located

within the host crystal and one in which it is located in a reservoir, usually taken to be the ground-state crystalline phase. This energy difference can be straightforwardly calculated by a first-principles total-energy method such as density-functional theory (DFT). Such an approach has afforded gain great insight into the equilibrium solubility of different dopants in many semiconductor hosts.[13]

It is important to realize that the above formalism is only strictly valid under conditions of thermodynamic equilibrium. In particular, the host+dopant system must be in thermal and chemical equilibrium with a reservoir of dopant atoms. Of course, no real system ever completely satisfies this requirement. A more practical requirement is that dopants are sufficiently mobile that different configurations can be adequately sampled, and equilibration reached, in a reasonable time.[13] This requirement is satisfied for some semiconductor growth methods but not all. For example, metal-organic chemical-vapor deposition is typically performed above 1000 °C. Such high temperatures are sufficient to ensure good equilibration of most dopants and other defects. But semiconductors are also grown at much lower temperatures, for example, using molecular-beam epitaxy (MBE), typically in the range 200–800 °C. At these temperatures dopants are much less likely to be mobile. Indeed, the growth by MBE of dilute magnetic semiconductors such as Mn-doped GaAs is performed in the range 200–300 °C specifically to *avoid* equilibration of the GaAs host and Mn dopants.

B. Trapping of dopants inside nanocrystals

Semiconductor nanocrystals can be grown by synthetic methods based on the solid, liquid, or gas phase. The most uniform crystallites are produced by liquid-phase colloidal chemistry, at temperatures that are generally below 350 °C, and even as low as room temperature. At these low temperatures the assumption of thermodynamic equilibration of the host+dopant system is unlikely to be valid for most materials. This is because diffusion is an thermally activated process, with a hopping rate $\nu_{\mathrm{diff}}=\nu_{\mathrm{diff}}^{0}\exp(-E_{\mathrm{diff}}/kT)$, where ν_{diff}^{0} is the bare attempt frequency (typically $10^{12}-10^{13}$ s^{-1}) and E_{diff} is the activation barrier. If diffusion is to be effective on the time scale of a nanocrystal growth experiment, a hopping rate of order 1 per second is required. At colloidal temperatures this can only be attained if the activation barrier is less than about 1.5 eV.

Measured activation barriers for most dopants in semiconductors are substantially larger than this. For example, the activation energy for diffusion of Mn dopants in bulk CdTe is 2.3–2.8 eV.[14] Such a large barrier implies negligible diffusion at colloidal growth temperatures. This fact motivates the first fundamental assumption of the trapped-dopant model: an impurity atom that occupies a substitutional site during colloidal nanocrystal growth will remain there as a "trapped dopant."

The validity of this assumption obviously depends on many details, not the least of which are the nanocrystal host material and the type of dopant atom. Indeed, there are interesting counterexamples—such as the reversible transformation under ambient conditions of CdSe nanocrystals, when exposed to Ag, to Ag_2Se nanocrystals.[15,16] But most experimental evidence supports the assumption of trapped dopants. For example, Cao and co-workers[17] have recently developed a method to control precisely the radial position of a Mn dopant inside a core/shell colloidal nanocrystal; this control would not be possible if significant Mn diffusion occurred during growth.

In the present work, DFT calculations are used to evaluate the validity of the trapped-dopant assumption for a set of candidate dopants in PbSe. Specifically, the diffusion barriers E_{diff} are calculated for a simple diffusion pathway in bulk PbSe. These barriers should be very similar to those in nanocrystalline PbSe, possibly with modifications near the surface. Dopants for which E_{diff} is larger than roughly 1.5 eV can be assumed to be trapped during growth under colloidal conditions. This criterion thus provides a first test of potential dopants in PbSe nanocrystals.

C. Adsorption of dopants on nanocrystals

If dopants cannot diffuse outward and escape from the interior of a nanocrystal then nor, by the same reasoning, can they diffuse inward to be incorporated from the growth solution. A plausible alternative is for dopants first to adsorb stably on the surface of the nanocrystal. This leads to the second fundamental assumption of the trapped-dopant model: if an adsorbed impurity remains bound for sufficiently long to be overgrown by additional host material then it will, in effect, be incorporated into the nanocrystal as a dopant.

This principle provides a simple starting point for evaluating the likelihood that a given impurity will be incorporated into a nanocrystal as a dopant. Of course, the details of the adsorption process may be quite complicated, for example, requiring first the dissociation of the impurity from a coordinating molecule; this issue will be discussed in Sec. II D. Nonetheless, an important prerequisite for satisfying the condition stated above is that the isolated impurity atom can adsorb on the nanocrystal surface with a sufficiently large binding energy. A rough estimate of "sufficiently large" can be obtained from the desorption rate of a single impurity, $\nu_{\mathrm{ads}}\exp(-E_{\mathrm{ads}}/kT)$. As for diffusion, ν_{ads} is typically of order $10^{12}-10^{13}$ s^{-1}, and so incorporation is possible at colloidal temperatures only if the adsorption energy E_{ads} is roughly 1.5 eV or larger.

In an earlier work, the calculated adsorption energies of a Mn impurity on different semiconductor hosts were shown to explain several experimentally observed trends in the dopability of nanocrystals.[6] For example, the calculated maximum adsorption energy of Mn on ZnSe ($E_{\mathrm{ads}}=4$ eV) was found to be much larger than on CdSe ($E_{\mathrm{ads}}=2$ eV). It was proposed in Ref. 6 that this difference accounts, in part, for the very different Mn concentrations attained experimentally in nanocrystals of ZnSe (0.45%) versus CdSe (0.14%) when similar growth and doping methods were used. It was also proposed that chemically induced changes in the shape of a ZnSe nanocrystal would result in different concentrations of incorporated Mn because the adsorption energy on the (111) and (110) facets is much smaller ($E_{\mathrm{ads}}\approx 1$ eV) than on the

(001) facet ($E_{ads} \approx 4$ eV). Experimentally, by increasing the Se:Zn ratio from 1:1 to 4:1, the concentration of incorporated Mn indeed increased by 30%. This increase was attributed to changes in the shape of the nanocrystal, which depends on the Se:Zn ratio.[6]

In the present work, DFT is used to calculate the adsorption energies of several candidate dopants on different surface facets of PbSe. The adsorption energies are calculated on clean PbSe surfaces, even though PbSe nanocrystals are in practice passivated by ligand molecules during the growth. This choice is motivated by a previous study of Mn impurity adsorption on CdSe in which it was found that calculated adsorption energies on clean and ligand-passivated surfaces were quite similar.[12] Qualitatively, dopants for which E_{ads} is larger than roughly 1.5 eV can be assumed to be stably adsorbed during growth under colloidal conditions. This criterion thus provides a second test of potential dopants in PbSe nanocrystals.

D. Competition for dopants from other agents

In the above discussion of adsorption, the dopants were treated as single atoms interacting solely with the nanocrystal surface. This treatment is too simplistic. The incorporation of dopants into nanocrystals is also affected by the presence of surfactants, which are routinely used to moderate the growth rate of the nanocrystals by passivating their surface.[6]

An explanation of the role played by surfactants in doping was proposed in Ref. 12 using a simple model and is easily illustrated using the example of Mn dopants and CdSe nanocrystals. A surfactant that binds strongly to surface Cd sites, such as tetradecylphosphonic acid (TDPA), also binds strongly to individual Mn atoms in the growth solution because Cd and Mn have the same chemical valence. Since the number of Mn atoms in solution is generally much smaller than the number of surfactant molecules, every Mn atom in solution can be assumed to be bound to a surfactant molecule. When one such impurity-surfactant complex approaches the nanocrystal surface it may, depending on the outcome of a competition for forming strong chemical bonds, undergo a process of dissociative adsorption. This leads to the third assumption of the trapped-dopant model: the impurity-surfactant complex must dissociate—either spontaneously or by thermal activation—as it nears the nanocrystal surface, allowing the separated surfactant molecule and impurity atom to find stable binding sites.

Although this principle is easily stated, any quantitative predictions based on it are unlikely to be definitive in view of the many degrees of freedom for dissociative adsorption of a large complex. Nevertheless, qualitative conclusions are possible if one restricts attention to just two aspects of dissociative adsorption: the transition state, and the relative energy of the initial and final states.

The most important feature of the transition state is the energy barrier E_a to dissociative adsorption. This barrier can play a central role in the impurity sticking probability and, therefore, in the efficiency of nanocrystal doping. For example, if the impurity atom is sufficiently strongly bound after dissociation, then its subsequent desorption rate is very low and the impurity sticking probability for this reaction pathway is simply $\exp(-E_a/kT)$. Thus, if E_a is large compared to kT then doping will be inefficient.

However, even spontaneous dissociation ($E_a=0$) does not necessarily imply efficient doping. If the impurity adsorption energy is smaller than the impurity-surfactant binding energy, then dopants may be delivered to the surface only to desorb back into solution. This possibility was investigated theoretically in Ref. 12 in a case study of Mn doping of CdSe nanocrystals in the presence of two different surfactants, TDPA and hexadecylamine (HDA). The key question is whether the Mn adsorption energy, calculated to be in the range $E_{ads}=1.4-2.5$ eV depending on the surface, is larger or smaller than the Mn-surfactant binding energy. For TDPA the Mn-surfactant binding energy is 5.9 eV, much larger than the adsorption energy. This strong binding provides an energetically downhill route for Mn dopants to desorb back into solution, consistent with experiments showing that no Mn is incorporated in CdSe nanocrystals when TDPA is used.[18] For the less aggressive surfactant HDA the Mn-surfactant binding energy is only 0.5 eV, much less than the adsorption energy. This weak binding blocks desorption of Mn back into solution, consistent with experiments showing successful doping of CdSe nanocrystals with Mn when HDA was used.[6]

In the present work, DFT is used to calculate the impurity-surfactant binding energies for several candidate impurities with different surfactants. A large binding energy, relative to the impurity adsorption energy on PbSe, should be viewed as unfavorable for doping. A small binding energy, while not a sufficient condition for favorable doping, thus provides a third test for choosing impurity-surfactant combinations for doping PbSe nanocrystals.

III. PbSe HOST AND CANDIDATE DOPANTS

In this work, the model of doping described above is applied to PbSe nanocrystals and a number of candidate dopants. As a host material, PbSe presents both scientific challenges for understanding doping and opportunities for technological applications. The crystal structure of PbSe is rocksalt, and hence its surface structure is very different from the II-VI zinc-blende and wurtzite materials for which earlier theoretical and experimental work established the importance of adsorption for doping.[6] For this reason, the earlier findings for II-VI zinc-blende nanocrystals—for example, that Mn adsorption is very stable on (001) surface facets and much less so on (110) and (111) facets—will not necessarily apply to PbSe.

Technologically, PbSe is an attractive material for several reasons. First, the Bohr radius of the exciton in PbSe, $a_B=46$ nm, is extremely large, indeed larger than for almost any other semiconductor. This means that a very wide range of nanocrystal sizes (with dimensions up to a_B) will exhibit quantum confinement. Such broad latitude is useful for both technological and research reasons: for example, relatively large nanocrystals have small surface-to-volume ratios, reducing the influence of surface states while still achieving quantum confinement of the carriers.

Second, bulk PbSe has a very small band gap (0.28 eV at room temperature). This means that the size quantization of

energy levels in PbSe nanocrystals can be tuned over a very wide spectral range in the important near- and mid-infrared regions (wavelengths from 900 nm to 2.3 μm).

Third, the band structure of PbSe is nearly unique in that the conduction and valence bands exhibit almost perfect mirror symmetry for low-energy (up to ~0.3 eV) excitations. This means that electron and hole masses are not only very light but also nearly equal, and hence that the exciton wave function has equal amplitude on the electron and hole. Confining both electron and hole states is advantageous for two reasons: (1) the resulting optical-absorption coefficient is high, which is important for photovoltaic applications. (2) The resulting energy spectra for electrons and holes remain quantized even at room temperature. For PbSe nanocrystal wires, this protects the advantages of the one-dimensional density of states (potentially important, for example, in thermoelectric applications) from thermal degradation.

A variety of candidate dopants are investigated in this work: light and heavy elements, potential donors and acceptors, and magnetic as well as nonmagnetic elements. Justification for the specific choices can be advanced on several grounds. Dopants that may act as donors or acceptors when substituting for the group-IV host cation (Pb) might plausibly include elements from group V (N, P, As, Sb, and Bi) and group III (B, Al, Ga, In, and Tl), respectively. Dopants with magnetic moments (Mn and Co) may be more readily detected experimentally, using electron paramagnetic resonance or magnetic circular dichroism. Finally, dopants already used for bulk PbSe include three acceptors (Cl, In, and Cd) and a donor (Tl).[19] In total, this list of candidates amounts to 14 potential dopants covering a wide range of physical size, valence, and magnetic properties.

IV. TRAPPING OF DOPANTS

A. Methods

A detailed study of how dopants diffuse in PbSe is far beyond the scope of this work. Instead, a simplified approach is adopted here in which each candidate dopant is assumed to be substitutional on the Pb site. A simple diffusion pathway is then assumed, one with an easily identified transition state. The energy of this transition state, relative to the initial state, then defines the energy barrier for dopant diffusion.

In bulk semiconductors the diffusion of substitutional impurities is often mediated by vacancies or interstitials. For colloidally grown semiconductor nanocrystals these defects are likely to be rare or absent. Thus dopant diffusion will be considered here to occur without vacancies or interstitials. One well-known diffusion mechanism of this type involves a simple "concerted-exchange" process in which the dopant atom and one of its nearest-neighbor Pb atoms swap places. For concerted exchange within bulk PbSe, the reaction pathway is likely to take the simple form depicted in Fig. 1. Qualitatively, the impurity and the Pb atom swap places by "circling around" the axis that connects the two nearest Se atoms. This axis is perpendicular to the (110) plane in Fig. 1 and hence the motion of the two exchanged atoms may be viewed as taking place within the (110) plane, although this need not be strictly true. Figure 1(d) shows the full potential-

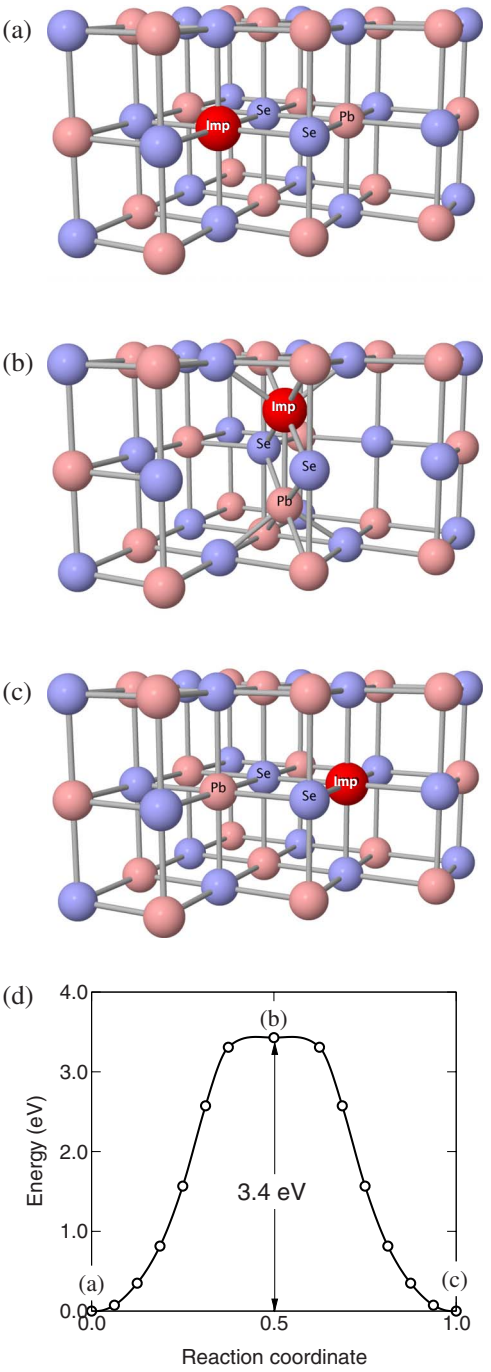

FIG. 1. (Color online) Concerted-exchange diffusion pathway for a substitutional impurity atom (large red atom) on a Pb site in bulk PbSe. (a) Initial state. (b) Transition state, assumed to be at the midpoint of the reaction pathway. (c) Final state. Ideal unrelaxed coordinates are shown here but full relaxation was performed in the calculations. (d) Theoretical potential-energy surface calculated for one example, Sb.

energy surface along this reaction pathway for one example (an antimony impurity) calculated using the nudged elastic-band method. Of special interest here is the transition state, located halfway along this reaction pathway as shown.

First-principles total-energy calculations were used to determine relaxed geometries and relative energies of the initial

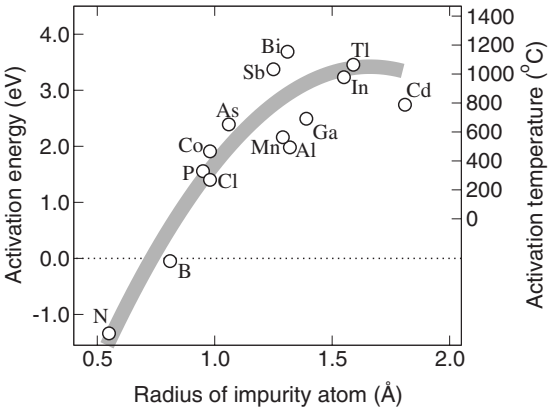

FIG. 2. Theoretical activation energies E_{diff} for diffusion of candidate dopants in bulk PbSe. The concerted-exchange diffusion pathway of Fig. 1 is assumed; the activation energy is the energy of the transition state relative to the energy of the initial state. Activation temperatures were calculated by assuming a reaction rate $\nu_{\mathrm{diff}}=1\ \mathrm{s}^{-1}$ and simple Arrhenius behavior $\nu_{\mathrm{diff}}=\nu_{\mathrm{diff}}^{0}\exp(-E_{\mathrm{diff}}/kT)$ with an attempt frequency $\nu_{\mathrm{diff}}^{0}=10^{13}\ \mathrm{s}^{-1}$. The curve is a guide to the eye.

state and transition state for each candidate dopant in PbSe. The calculations were performed in a 64-atom supercell with $2\times2\times2$ Monkhorst-Pack sampling at the theoretical lattice constant, 6.19 Å, of bulk PbSe. All atomic positions were relaxed until the largest force component on every atom was below 0.05 eV/Å. Full relaxation at the transition state, Fig. 1(b), was made possible by an extra mirror symmetry that constrains the four labeled atoms to their common mirror plane. Total energies and forces were calculated within the generalized-gradient approximation of Perdew, Burke, and Ernzerhof (PBE) to DFT using projector-augmented-wave potentials, as implemented in VASP.[20,21] The plane-wave cutoff for all calculations was 270 eV. The Mn and Co calculations were performed with spin polarization.

B. Results

Figure 2 shows the resulting theoretical activation energies E_{diff}. Although the 14 candidate dopants have a wide range of physical, electronic, and magnetic properties, their respective activation energies depend, with surprising regularity, on a single property—their size. By size we mean here the dopant's radius, defined as half the DFT bond length of a molecular dimer consisting of two dopant atoms, e.g., Mn_2. Figure 2 show a simple and physically sensible trend: larger dopants have larger activation energies.

Twelve of the 14 candidate dopants have substantial activation energies in the range 1.5–4.0 eV. (The two smallest dopants, boron and nitrogen, have negative barriers, indicating that the assumption of a substitutional cation site was unrealistic for these atoms.) This range of energies corresponds to activation temperatures in the range 300–1200 °C. By comparison, the colloidal synthesis of PbSe nanocrystals is carried out at growth temperatures between 150 and 250 °C, well below the range of activation temperatures.[22] This implies that most of the 14 candidate dopants—those with a radius approximately 1 Å or larger—will remain kinetically trapped on Pb substitutional sites during the colloidal growth process.

V. ADSORPTION OF DOPANTS

A. Methods

The adsorption of a dopant on the surface of a nanocrystal depends on the structure and chemistry of that surface—that is, on the available binding sites and their corresponding binding energies. These vary greatly for different materials, and it is only possible to make useful predictions on a case-by-case basis. Hence, our earlier finding[6] of selective adsorption on zinc-blende II-VI nanocrystals—for example, the (001) surface of ZnSe provides much more favorable binding than the (111) or (110) surfaces—does not in any way imply similar behavior for rocksalt VI-VI nanocrystals of PbSe. The different crystal structure, surface structure, and surface chemistry of PbSe require a new investigation.

In this section we explore adsorption on PbSe by addressing four questions. (1) Is there a general trend governing the binding energies of dopants on a given facet of PbSe? (2) Do the facets of PbSe nanocrystals show selective behavior, with one facet offering more favorable binding sites than the others? (3) How do dopants adsorb at the edges where two planar facets are joined? (4) How do dopants adsorb on a partially or completely "roughened" nanocrystal, that is, one whose surface does not consist of crystallographically well-defined facets?

We address the first two of these questions by treating adsorption on the low-index surfaces PbSe(001), PbSe(110), and PbSe(111). These are the facet orientations that comprise most of the exposed surface of the quasispherical PbSe nanocrystal with diameter 5 nm shown in Fig. 3. As discussed in Sec. II C, we consider adsorption of impurity atoms on the clean PbSe surfaces, despite the fact that PbSe nanocrystals are passivated by organic ligands during their growth. The PbSe(001) and PbSe(110) surfaces are unreconstructed but the polar PbSe(111) surface reconstructs to lower its surface energy. Various reconstruction models have been proposed in the literature.[23] Here we assume a 2×2 octupolar reconstruction analogous to that found experimentally on NiO(111).[24,25] This reconstruction can be realized with both *A* (Pb-polar) and *B* (Se-polar) terminations; the surface energies are very close (within 1 meV/Å^2), with the *A* termination lower.

We address the third and fourth questions by examining the possible adsorption sites near the edge where two or more planar facets meet. Figures 3(c) and 3(d) show that there are many such sites on a typical 5 nm nanocrystal. These sites are of just two types: a step-edge site and a corner site, with respect to the flat (001) surface, as illustrated by the upper green and red adsorbates in Fig. 3(d), respectively. Because of the underlying rocksalt crystal structure, the local coordination of these two sites is identical to the local coordination on the flat (110) and flat (111) facets, respectively, as shown by lower green and red adsorbates. Therefore we anticipate that the adsorbate binding energies

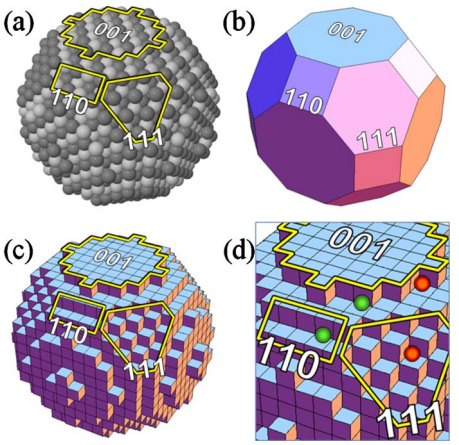

FIG. 3. (Color online) Surface morphology of a quasispherical PbSe nanocrystal with diameter 5 nm in three equivalent representations. (a) Pb atoms are dark gray and Se atoms are light gray. Many of the atoms at the surface belong to the (001), (110), or (111) planar facets indicated by the yellow outlines. (b) Polyhedron showing a simplified view of the surface facets for clarity. [(c) and (d)] Cuboid representation showing the near equivalence of the (001) step-edge site and the (110) planar site (green adsorbates), and of the (001) corner site and the (111) planar site (red adsorbates).

at the step-edge and corner sites should be quite close to the energies at the flat (110) and (111) surfaces.

To compute the binding energies of impurity atoms on flat and stepped surfaces we used 2×2 surface supercells of symmetric slabs consisting of either five atomic layers [for (001) and (111)*A*] or six atomic layers [for (110)], and 2×2 sampling of the surface Brillouin zone. The outermost two layers of PbSe and the adsorbate position were relaxed until the largest force component on every atom was below than 0.05 eV/Å.

B. Results

Figures 4–6 show the resulting adsorbate binding energies on the three low-index PbSe surfaces. These binding energies are defined with respect to the infinitely separated adsorbate atom and relaxed surface. The Mn and Co atomic energies

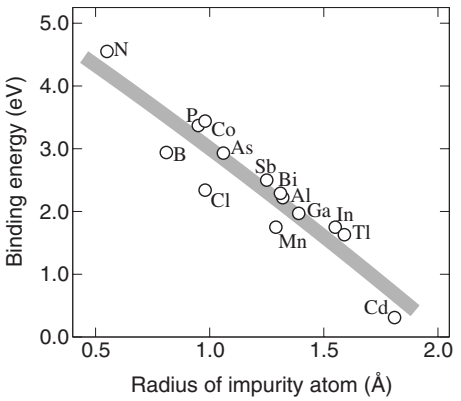

FIG. 4. Binding energies of candidate dopants adsorbed on the PbSe(001) surface. The curve is a guide to the eye.

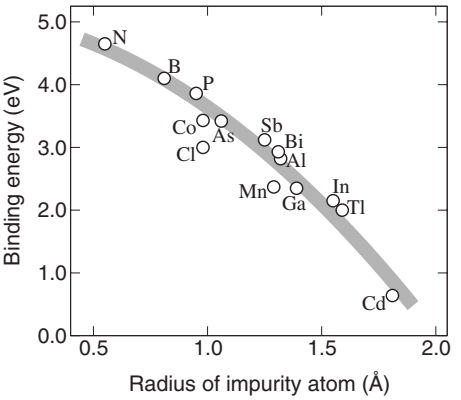

FIG. 5. Binding energies of candidate dopants adsorbed on the PbSe(110) surface. The curve is a guide to the eye.

are for spin-polarized atoms; all others are for nonpolarized atoms.

All three surfaces reveal the same trend: larger dopants have smaller binding energies. The range of binding energies is quite large, from approximately 5 eV for nitrogen to less than 1 eV for cadmium. The range of energies for the more typical dopants, on all three surfaces, is approximately 2–4 eV. The correlation between atomic size and surface binding energy is quite close, especially for the (001) and (110) surfaces. The origin of this correlation is physically simple: smaller dopants can approach closer to the surface and thereby maximize their coordination to surface atoms. Figure 7 shows the distance, at equilibrium, of each adsorbate above the PbSe(110) surface plane. These distances are, for the most part, within a few tenths of an angstrom of those predicted by a simple hard-sphere model of atoms.

For adsorption at step-edge and corner sites, the assertion was made above that these sites should offer binding energies similar to the flat (110) and (111) surfaces, respectively. This assertion is tested numerically in Fig. 8, which compares the DFT binding energies at the step-edge and the flat (110) surface. To within a few percent they are indeed very close.

According to the discussion in Sec. II C, the minimum adsorbate binding energy required for dopant incorporation is roughly 1.5 eV. Virtually all of the candidate dopants ex-

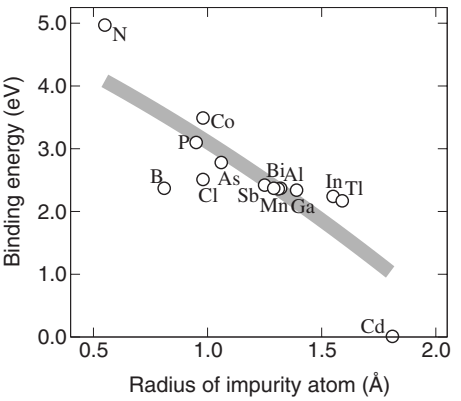

FIG. 6. Binding energies of candidate dopants adsorbed on the PbSe(111)*A* surface. The curve is a guide to the eye.

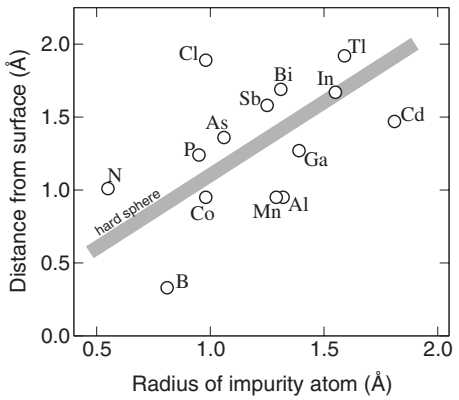

FIG. 7. Equilibrium distance from the surface plane of candidate dopants adsorbed on the PbSe(110) surface. The curve shows the result for hard spheres with no relaxation.

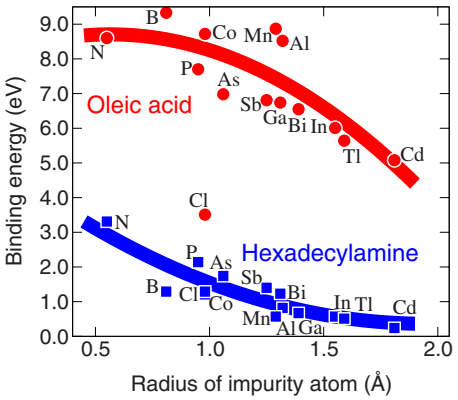

FIG. 9. (Color online) Binding energies of candidate dopants to oleic acid (circles) and hexadecylamine molecules (squares). The curves are guides to the eye.

ceed this threshold on all three flat surfaces. Cadmium, the largest dopant studied here, is the sole exception. At surface sites that are not part of a planar facet the binding energies are very similar and so a similar conclusion holds. The surface of any PbSe nanocrystals of arbitrary shape consists of only these three basic types of sites. Therefore almost all of the 14 candidate dopants—those with a radius approximately 1.5 Å or smaller—will remain stably adsorbed somewhere on the PbSe nanocrystal surface sufficiently long to be incorporated during the growth.

VI. COMPETITION FROM OTHER AGENTS

A. Methods

Colloidal PbSe nanocrystals and nanowires are most commonly prepared using a variety of stabilizing agents and solvents. These include oleic acid, hexadecylamine, trioctylphosphine, tetradecylphosphonic acid, and others.[22] If any of these agents binds aggressively to potential dopant atoms during the synthesis, then doping will be strongly suppressed or pre-empted. To investigate this possibility we focus on the binding of candidate dopants to two of these agents: oleic acid and hexadecylamine.

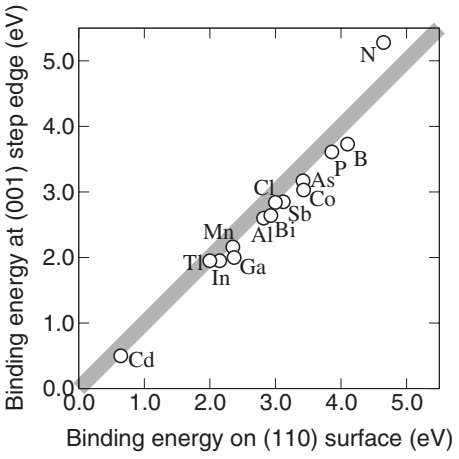

FIG. 8. Comparison of binding energies of candidate dopants adsorbed at a PbSe(001) step to binding energies on the flat PbSe(110) surface. The diagonal line denotes equal energies.

During the synthesis of undoped PbSe nanoparticles, oleic acid reacts with PbO to form a lead oleate precursor. The structure of lead oleate is relatively simple, consisting of a Pb atom centrally coordinated by two oleic acid molecules. Oleic acid is a long-chain fatty acid molecule, $CH_3(CH_2)_7CH{=}CH(CH_2)_7COOH$, which binds to other species at its COOH head group. For computational convenience we replace the long hydrocarbon tail by a single hydrogen atom to make the much simpler formic acid, HCOOH, which has the same active head group as oleic acid. We assume that each candidate dopant, for example, Mn forms a complex, $(HCOO)_2Mn$, whose structure is analogous to that of lead oleate. We define the binding energy with respect to the separated constituents of this complex.

The shape of PbSe nanocrystals and nanowires can be controlled by adding long-chain primary amines such as hexadecylamine, dodecylamine, and oleylamine to the reaction mixture.[22] These molecules act as cosurfactants by passivating the nanocrystal surface during the synthesis. Consequently they may also, in principle, bind pre-emptively to dopant atoms in the reaction mixture. We focus here on HDA, $C_{16}H_{33}NH_2$, which consists of a NH_2 head group and a long hydrocarbon tail. For computational convenience we truncate this molecule to the much simpler methylamine, CH_3NH_2, which has the same active head group.

B. Results

Figure 9 shows the resulting binding energies of dopant atoms to oleic acid and to hexadecylamine. The two molecules show quite different behavior. Oleic acid is an aggressive agent with very large binding energies in the range 5–10 eV (except for Cl, the single outlier). Hexadecylamine is a much weaker agent with binding energies below 2 eV for all dopants except N.

These energies should be compared with the range of adsorbate binding energies on the PbSe nanocrystal surface, typically 2–4 eV, discussed in Sec. V. This range is larger

than the molecular binding energies offered by hexadecylamine; consequently, hexadecylamine can be anticipated not to interfere with nanocrystal doping. Oleic acid, on the other hand, offers much more favorable binding for most dopants than does the PbSe nanocrystal surface. This implies that the use of oleic acid—a standard part of PbSe nanocrystal synthesis—will strongly suppress or even preempt doping.

VII. CONCLUSIONS

The goal of this work is twofold: to investigate the validity and general implications of the trapped-dopant model for PbSe nanocrystals and to identify specific candidate dopants that show the best potential for doping PbSe nanocrystals. The validity of the trapped-dopant model for a particular materials system hinges on whether impurities can diffuse. In Sec. IV we showed that most dopant atoms are kinetically trapped in PbSe at standard colloidal temperatures and hence cannot easily diffuse. More quantitatively, dopants with radius roughly 1 Å or larger will remain immobile at temperatures up to roughly 250 °C. A trapped-dopant model is therefore appropriate for most dopants under these conditions.

The most important implication of this trapping is clear: without diffusion, dopants can only be incorporated if they first adsorb stably on the surface. We showed in Sec. V that dopants on PbSe follow a simple trend that is opposite to trapping inside the nanocrystal, namely, larger dopants have *smaller* binding energies on the surface. More quantitatively, dopants with radius roughly 1.5 Å or smaller will remain bound to the surface for sufficiently long to be overgrown and thus incorporated.

Satisfying both of these criteria—for interior trapping and for surface adsorption—requires dopants within a rather narrow range of sizes, between 1.0 and 1.5 Å. Of the 14 candidates investigated in this work roughly half fall inside this range, and several others are close enough to be plausibly included.

Finally, we showed in Sec. VI that oleic acid, a standard component of PbSe nanocrystal synthesis, very likely preempts doping by strongly binding to impurity atoms. A new synthesis protocol designed to avoid this problem will be an important step toward successful doping of PbSe nanostructures.

ACKNOWLEDGMENTS

Many helpful conversations are gratefully acknowledged with Mao-Hua Du, Alexander Efros, Edward Foos, David Norris, and Joseph Tischler. This work was supported by the Office of Naval Research. Computations were performed at the DoD Major Shared Resource Center at AFRL.

[1] D. J. Norris, N. Yao, F. T. Charnock, and T. A. Kennedy, Nano Lett. **1**, 3 (2001).
[2] C. A. Stowell, R. J. Wiacek, A. E. Saunders, and B. A. Korgel, Nano Lett. **3**, 1441 (2003).
[3] K. Somaskandan, G. M. Tsoi, L. E. Wenger, and S. L. Brock, Chem. Mater. **17**, 1190 (2005).
[4] N. S. Norberg, K. R. Kittilstved, J. E. Amonette, R. K. Kukkadapu, D. A. Schwartz, and D. R. Gamelin, J. Am. Chem. Soc. **126**, 9387 (2004).
[5] J. D. Bryan and D. R. Gamelin, Prog. Inorg. Chem. **54**, 47 (2005).
[6] S. C. Erwin, L. J. Zu, M. I. Haftel, Al. L. Efros, T. A. Kennedy, and D. J. Norris, Nature (London) **436**, 91 (2005).
[7] G. M. Dalpian and J. R. Chelikowsky, Phys. Rev. Lett. **96**, 226802 (2006).
[8] M.-H. Du, S. C. Erwin, A. L. Efros, and D. J. Norris, Phys. Rev. Lett. **100**, 179702 (2008).
[9] G. M. Dalpian and J. R. Chelikowsky, Phys. Rev. Lett. **100**, 179703 (2008).
[10] J. Li, S.-H. Wei, S.-S. Li, and J.-B. Xia, Phys. Rev. B **77**, 113304 (2008).
[11] D. J. Norris, Al. L. Efros, and S. C. Erwin, Science **319**, 1776 (2008).
[12] M.-H. Du, S. C. Erwin, and Al. L. Efros, Nano Lett. **8**, 2878 (2008).
[13] C. G. Van de Walle and J. Neugebauer, J. Appl. Phys. **95**, 3851 (2004).
[14] N. Y. Jamil and D. Shaw, Semicond. Sci. Technol. **10**, 952 (1995).
[15] D. H. Son, S. M. Hughes, Y. Yin, and A. Paul Alivisatos, Science **306**, 1009 (2004).
[16] R. D. Robinson, B. Sadtler, D. O. Demchenko, C. K. Erdonmez, L.-W. Wang, and A. P. Alivisatos, Science **317**, 355 (2007).
[17] Y. Yang, O. Chen, A. Angerhofer, and Y. C. Cao, J. Am. Chem. Soc. **128**, 12428 (2006).
[18] F. V. Mikulec, M. Kuno, M. Bennati, D. A. Hall, R. G. Griffin, and M. G. Bawendi, J. Am. Chem. Soc. **122**, 2532 (2000).
[19] V. Kaidanov and Y. I. Ravich, Usp. Fiz. Nauk **145**, 51 (1985).
[20] G. Kresse and J. Hafner, Phys. Rev. B **47**, 558 (1993).
[21] G. Kresse and J. Furthmüller, Phys. Rev. B **54**, 11169 (1996).
[22] K. S. Cho, D. V. Talapin, W. Gaschler, and C. B. Murray, J. Am. Chem. Soc. **127**, 7140 (2005).
[23] C. Fang, M. A. van Huis, D. Vanmaekelbergh, and H. W. Zandbergen, ACS Nano **4**, 211 (2010).
[24] D. Wolf, Phys. Rev. Lett. **68**, 3315 (1992).
[25] A. Barbier, C. Mocuta, H. Kuhlenbeck, K. F. Peters, B. Richter, and G. Renaud, Phys. Rev. Lett. **84**, 2897 (2000).